Modeling of Optical Scattering in Advanced LIGO

Hunter Rew, Mentor: Joseph Betzwieser

November 3, 2014

Abstract

In a quantum limited sensitivity interferometer such as LIGO, light which scatters from an optic can introduce noise in the phase measurement at the antisymmetric port, as well as become a significant source of power loss. By measuring power seen by a camera or photodiode in a well defined position, outside of the beam path, one can use the incident light in order to model the total amount of light scattered from the optic. We have used the bidirectional reflectance distribution function on data obtained from photodiodes along the beam tubes baffles to model scattering from LIGOs test masses during each alignment since the first transmission of Advanced LIGO. This data acquisition and analysis has been automated for ease of future analysis. We have also experimentally determined 8 and 12 bit monochromatic count to Watt conversion factors for the Basler Ace 100gm cameras, currently used to monitor light within the interferometer, so that archived images may be used as a data source for the model.

Contents

1 Introduction

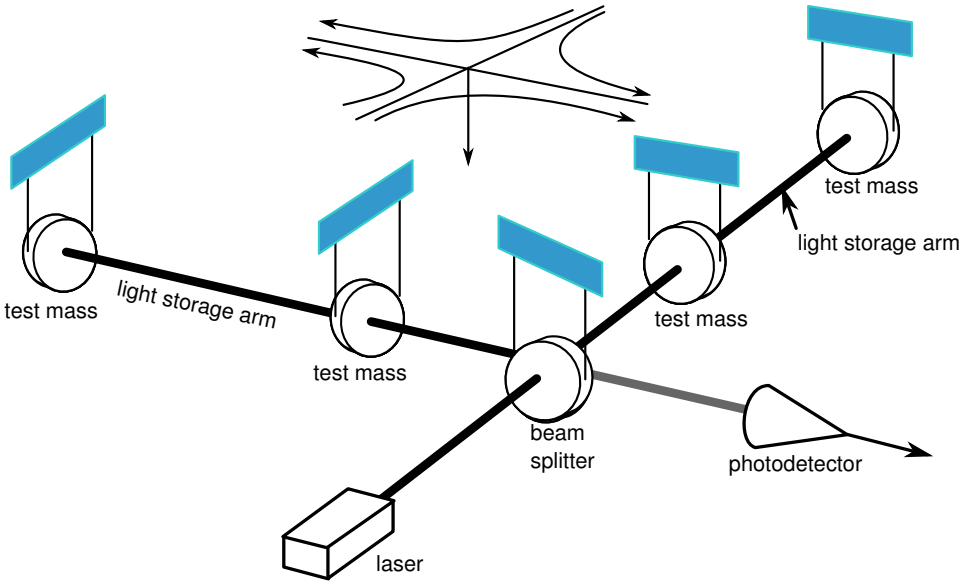

Figure 1: Diagram of a laser interferometer.

The Laser Interferometer Gravitational-Wave Observatory (LIGO) contains two Fabry-Perot cavities as seen in Figure 1 (labeled "light storage arms"). As light reflects between two test masses, a small percentage is scattered in an unintended direction due to surface imperfections. This scattering results in power loss and noise in the interferometer (IFO) which must be either accounted for or corrected [6]. Measuring optical scattering requires a power measurement of the light scattered to a known area, distance, and angle. This can be accomplished directly either through the use of a camera with a known conversion from power incident on the lens to intensity of light in the image or with a photodiode (PD). The scatter is measured by the Bidirectional Reflectance Distribution Function (BRDF) and is given by [7]:

$$BRDF = \frac{P_s}{\Omega \times P_i \times \cos(\theta_s)} \tag{1}$$

It is a measure of the ratio of power which is scattered (P_s) per solid angle (Ω) to power incident (P_i) on the reflecting surface. The solid angle is calculated as:

$$\Omega = \frac{A}{L} \tag{2}$$

Where A is the area of the surface and L is the distance from the point of scatter. This is a measure of the relative size of the area as seen from the point of scatter. Figure 2 shows how light reflects from an imperfect surface, as well as the scattered beams that the BRDF represents.

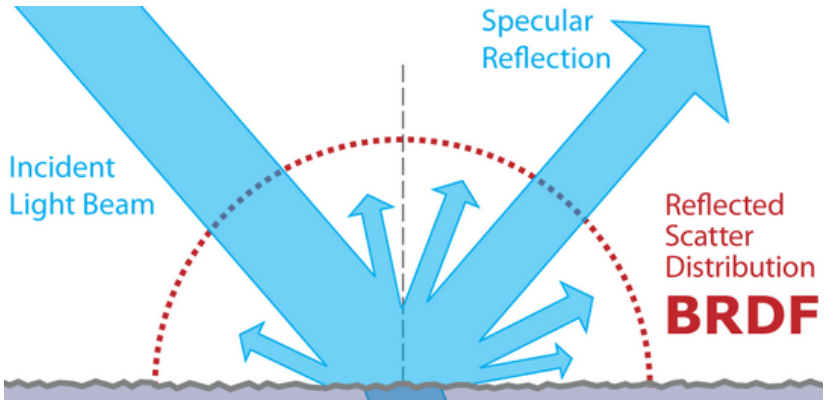

Figure 2: How light scatters from an imperfect surface [1].

2 Camera CCD Calibrations

There are cameras attached to viewports throughout the IFO aimed at specific optics such as the input mode cleaner (IMC), input test masses (ITMs), and end test masses (ETMs). One can determine where light is being scattered through analysis of the images from these cameras, however, the images alone can not tell how much light is being shown. To calculate this, one must know how the cameras CCD converts incident light to a pixel value at a given exposure. Then a conversion factor can be written in the form

$$\frac{Power(W) \times Exposure(\mu s)}{Intensity} = constant \tag{3}$$

where Intensity is the sum of pixel values. Thus, the power incident on the CCD can be calculated as some constant multiplied by the total light intensity per microsecond of exposure.

3 Calibration Measurement Equipment and Procedures

To begin, we installed a camera facing the Y-arm ETM with a beamsplitter to reflect 50% of the incoming light towards a PDA100A, connected to channel L1:LSC-Y_EXTRA_AI_2, in order to measure the power reaching the CCD [2]. This, however, had inherent problems, since the area of the photodetector (PD) is much (roughly 7 times) larger than the area of the CCD. In the end, this merely gave us an upper limit on the incident power, as we knew the PD was at least receiving as much light as the CCD, but could potentially receive several times more.

Our experimental setup is illustrated in Figures 3 and 4. When the beam reaches the first lens, it diverges to spread out the power. A pinhole sized beam is then allowed through the iris before reaching the converging lens, where it will be focused to a point on both the CCD and PD. We used this setup to start at a $4\mu s$ exposure, then increasing exposure in intervals until the image was nearly saturated. At this point we would decrease the power supplied to the laser in order to continue to longer exposures. Once we reached the point where the lasers power couldn't be reduced further, the ND filter was added to reduce the power to the CCD and PD by a factor of 10. With this method we were able to span from 4 to $1200\mu s$, at powers from 8.2 to $1.6\mu W$. Each power reading carried an uncertainty of $\pm 100nW$, which also limited how far we could reduce the power. 12 bit and 8 bit monochromatic data were taken for each exposure and power setting.

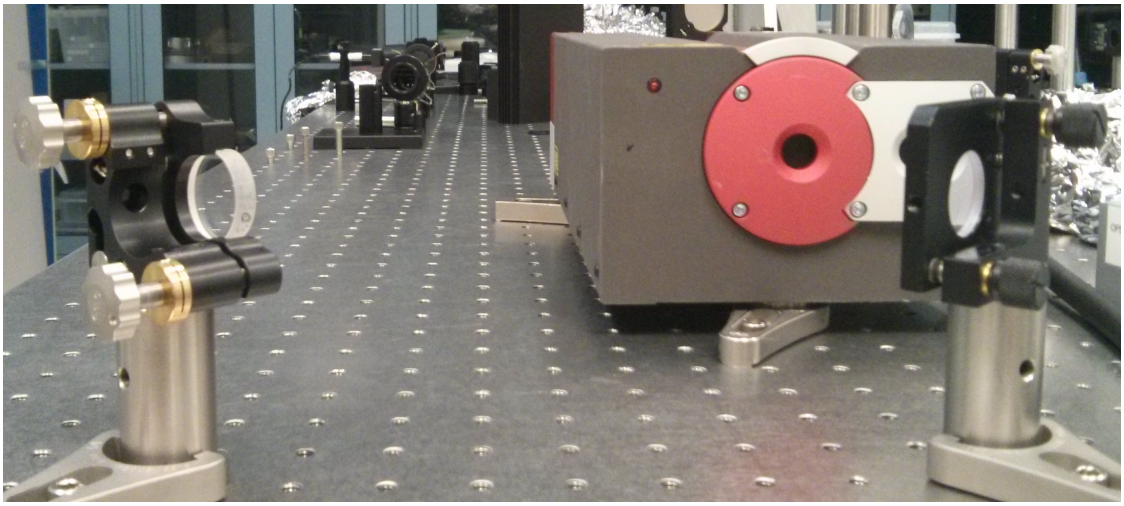

Figure 3: Infrared laser with two mirrors to control its path towards the camera.

We built a new setup in the optics lab, as shown in figures 1 and 2, consisting of the following:

- Innolight Prometheus 50NE laser
- Innolight Prometheus line power supply (not pictured)
- 2 infrared mirrors
- 30 mm diverging IR lens
- 65 mm converging IR lens
- lever controlled iris
- NE10A absorptive ND filter
- Thor Labs CM1-BS015 beam splitter
- Ophir NOVA laser power meter
- Basler acA640-100gm camera.

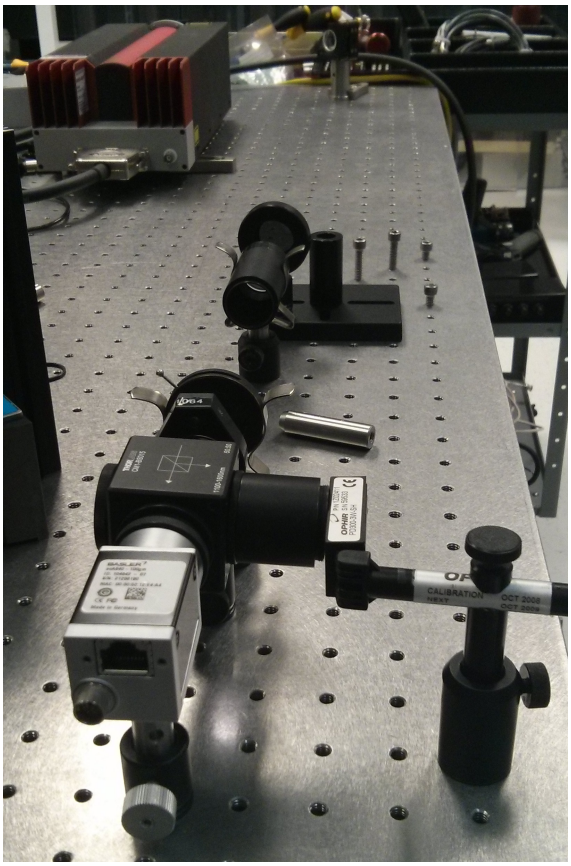

Figure 4: From front to back: camera, power meter, beamsplitter, 65mm lens, iris, -30mm lens, ND filter

4 Calibration Results and Analysis

Figure 5: 8 bit calibrations vs exposure on a logarithmic scale. Fluctuations in the calibration at lower exposures could be the result of noise fluctuations, as the sum of the pixel values is smaller compared to the noise.

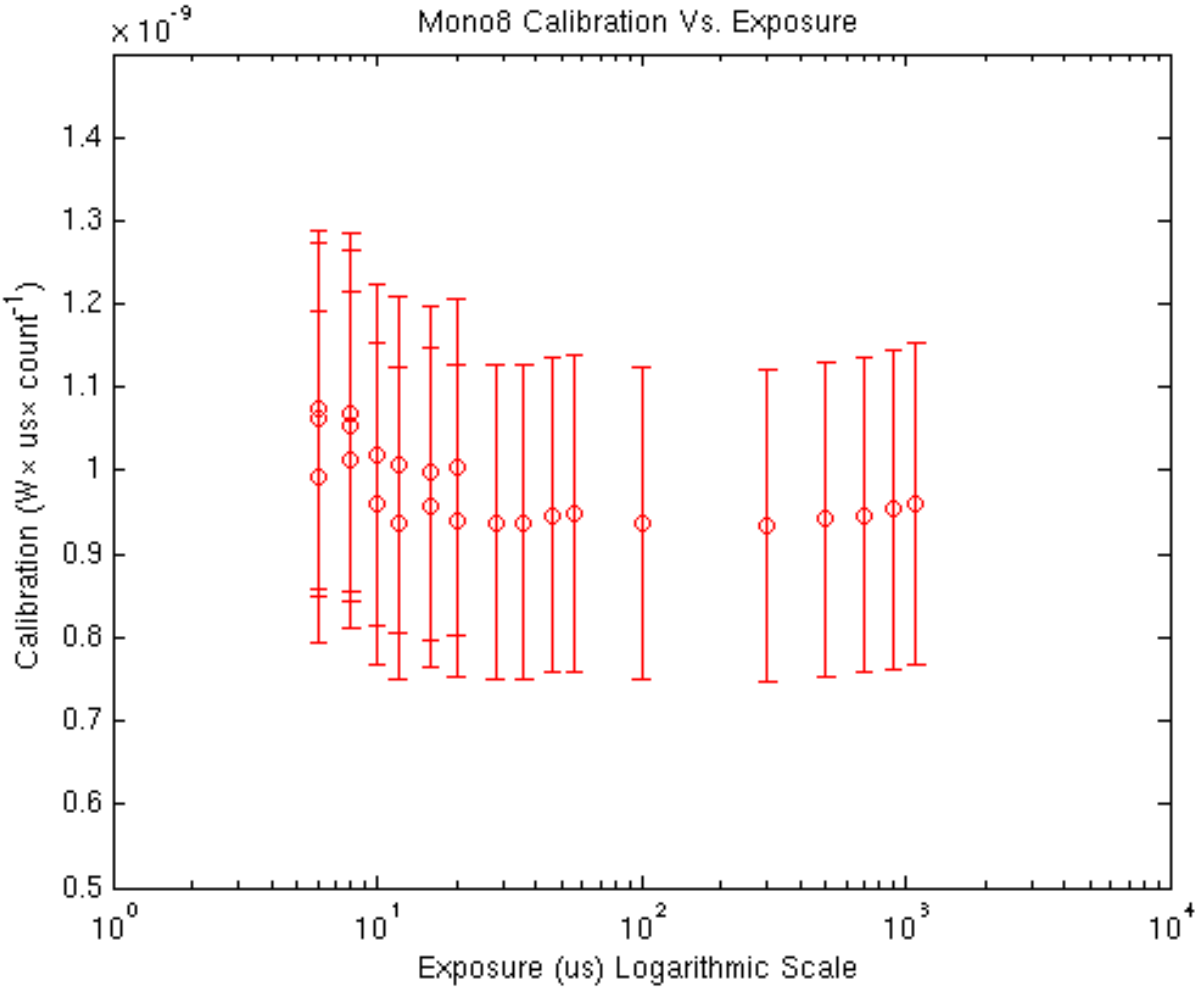

Because the ratio between exposure and pixel sum is constant at a given power, we were able to remove noise from each image by choosing a reference image at each power, and subtracting it from all other images at that power. A remaining image now represents an exposure equal to the difference of the images which it came from, with less noise than either. Plots of the 12 and 8 bit calibrations, calculated from Equation 3, are given in figures 5 and 6. For the 8 bit images, the mean calibration is $9.8 \times 10^{-10} W \cdot \mu s \cdot p_i^{-1}$, where p_i is the sum of the pixel values, or intensities. The standard deviation is $0.5 \times 10^{-10} W \cdot \mu s \cdot p_i^{-1}$. This is within the upper limit of the values measured by our camera and PDA100A, $1.4 \pm 0.2 \times 10^{-9} W \cdot \mu s \cdot p_i^{-1}$, where the uncertainty is the total fluctuation seen across all measurements. The mean calibration for the 12 bit images is $5.9 \times 10^{-11} W \cdot \mu s \cdot p_i^{-1}$ with a standard deviation of $0.3 \times 10^{-11} W \cdot \mu s \cdot p_i^{-1}$, roughly 16 times smaller than the 8 bit calibration, as would be expected. Error bars in the plots are presented as 20% due to differences in readings from different power meter heads.

Figure 6: 12 bit calibrations vs exposure on a logarithmic scale.

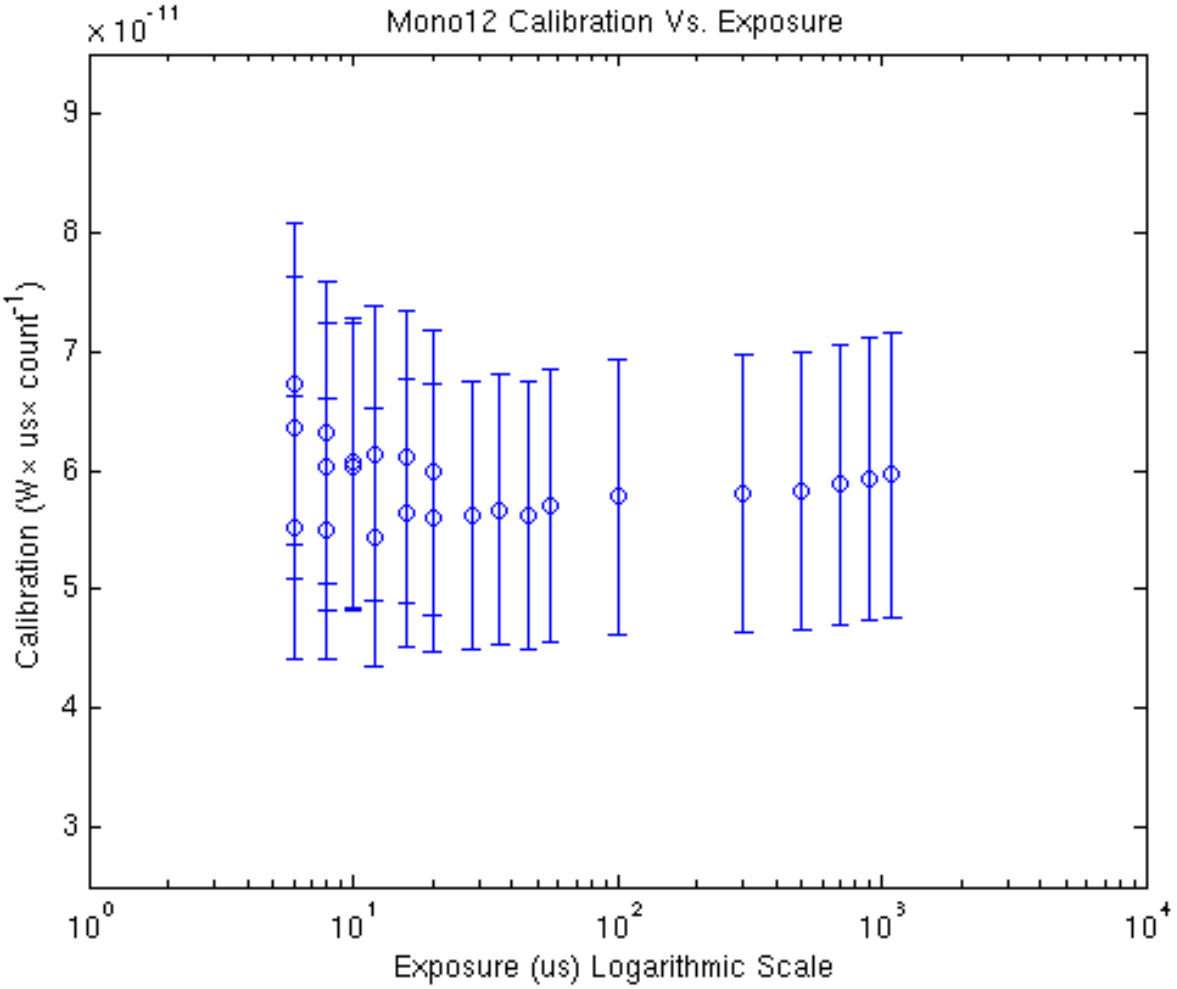

5 Baffle Photodiodes

Advanced LIGO contains structures called baffles between the test masses designed to block light scattered at specific angles from recombining with the main beam. There are 16 PDs within the beam tube baffles, 4 on each baffle, in order to aid in the initial alignment of the IFO as well as measure light scattered from TMs during alignment. The PDs are located around each baffle hole, directly in front of each TM within the Fabry-Perot cavity. A reading on a PD during a full lock gives the scattered power, P_s, which is calculated as:

$$P_s = \frac{V_s}{R \times T \times G} \tag{4}$$

where V_s is the voltage induced on the PD, R is the responsivity of the PD in A/W, T is the transimpedance of the PD in Ohms, and G is the dimensionless gain of the PD. By knowing the scattered power, the solid angle of the PD, Ω, its angle relative to the incident beam, θ_s, as well as the power of the incident beam, P_i, one can calculate the BRDF from Equation 1.

6 Baffle Photodiode Data Acquisition Procedures

6.1 Power Scattered to Photodiodes

PD voltages are taken from channels of the form $L1 : AOS - *TM* * \_BAFFLEPD\_ * \_VOLTS$, qhere $*TM*$ is the optic the baffle is attached to, including ITMX, ETMX, ITMY, and ETMY. The second $*$ can have a value of 1,2,3, or 4, indicating the PD. These channels output Volts. The power scattered to the PD, P_s, is calculated from the median voltage scattered to the PD as shown in Equation 4. Gain is taken from channels of the form $L1 : AOS - *TM* * \_BAFFLEPD\_ * \_GAIN$. Transimpedance is 20 kΩ, and responsivity is 0.25 ± 0.05 (A/W) [3]. Uncertainty in voltage for each lock is defined as the standard deviation of voltages throughout the lock. Uncertainty in the power scattered to each PD is calculated as a function of the uncertainties in responsivity and voltage as

$$(\Delta P_s)^2 = (\frac{1}{R \times T \times G})^2 (\Delta V_s)^2 + (\frac{V_s}{R^2 \times T \times G})^2 (\Delta R)^2 \tag{5}$$

The voltage offset is taken as the channel value at least 8 minutes before each lock.

6.2 Power Build Up in the Fabry-Perot Cavities

Power incident on each optic is calculated from the median value from the $L1 : LSC-POP\_A\_LF\_OUTPUT$ channel during each lock. This channel is the pick off from the power recycling cavity before the beam splitter and outputs Watts. After the laser passes through the beamsplitter, 50% of this power reaches each ITM. Power build up in each Fabry-Perot cavity is calculated as [6]

$$P_{cavity} = P_{ITM} \times \frac{2F}{\pi} \tag{6}$$

where $F = 416$ is the cavity finesse. The offset is taken as the value of $L1 : LSC-POP\_A\_LF\_OFFSET$, about 3.129 W. The uncertainty in cavity power for a lock is defined as the standard deviation of values during the lock.

6.3 When Data is Taken

We've defined the IFO to be in full lock (more or less arbitrarily) when the normalized output of the power recycling cavity, taken from the $L1 : LSC-POP\_A\_LF\_NORM\_MON$ channel, surpasses 20 for a duration of at least 30 minutes. This provides 84 locks. Reducing this duration to 15 minutes results in 155 locks with larger standard deviations.

6.4 Calculation of the BRDF

Solid angle is calculated from Equation 2 with $A = 100mm^2$ [3] as the area of the PD and $L = 4000mm$ as the approximate distance from the PD to the optic it is facing. Scatter angles are calculated from the measurements given in DCC document D1200296-v5 [5]. Uncertainty in the BRDF values is calculated as a function of the uncertainties in scattered power and incident power as:

$$(\Delta BRDF)^2 = (\frac{1}{\Omega \times P_i \times \cos(\theta_s)})^2 (\Delta P_s)^2 + (\frac{P_s}{\Omega \times P_i^2 \cos(\theta_s)})^2 (\Delta P_i)^2 \tag{7}$$

7 Baffle Photodiode Data Analysis

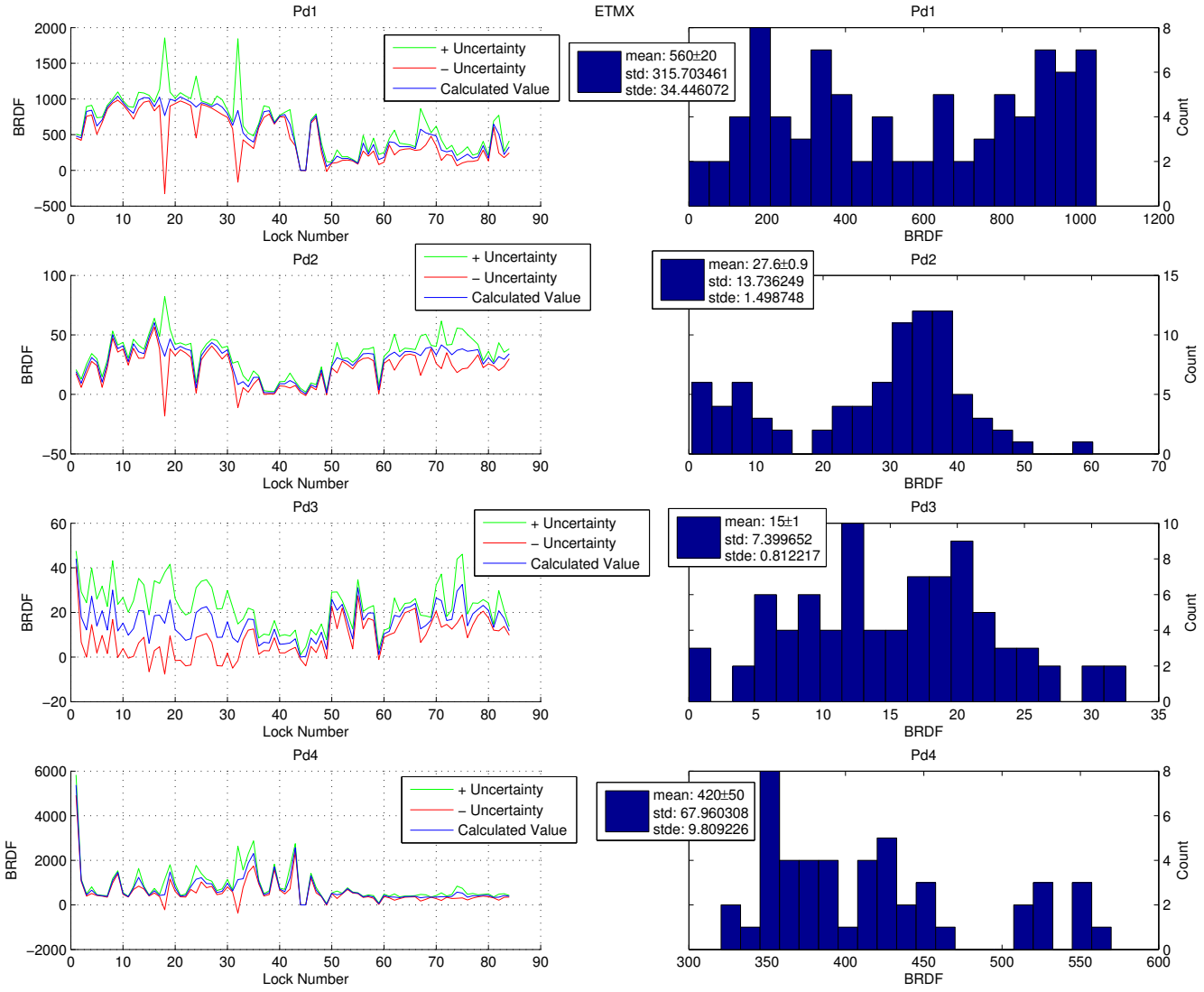

Figure 7: ETMX BRDFs and distribution by lock

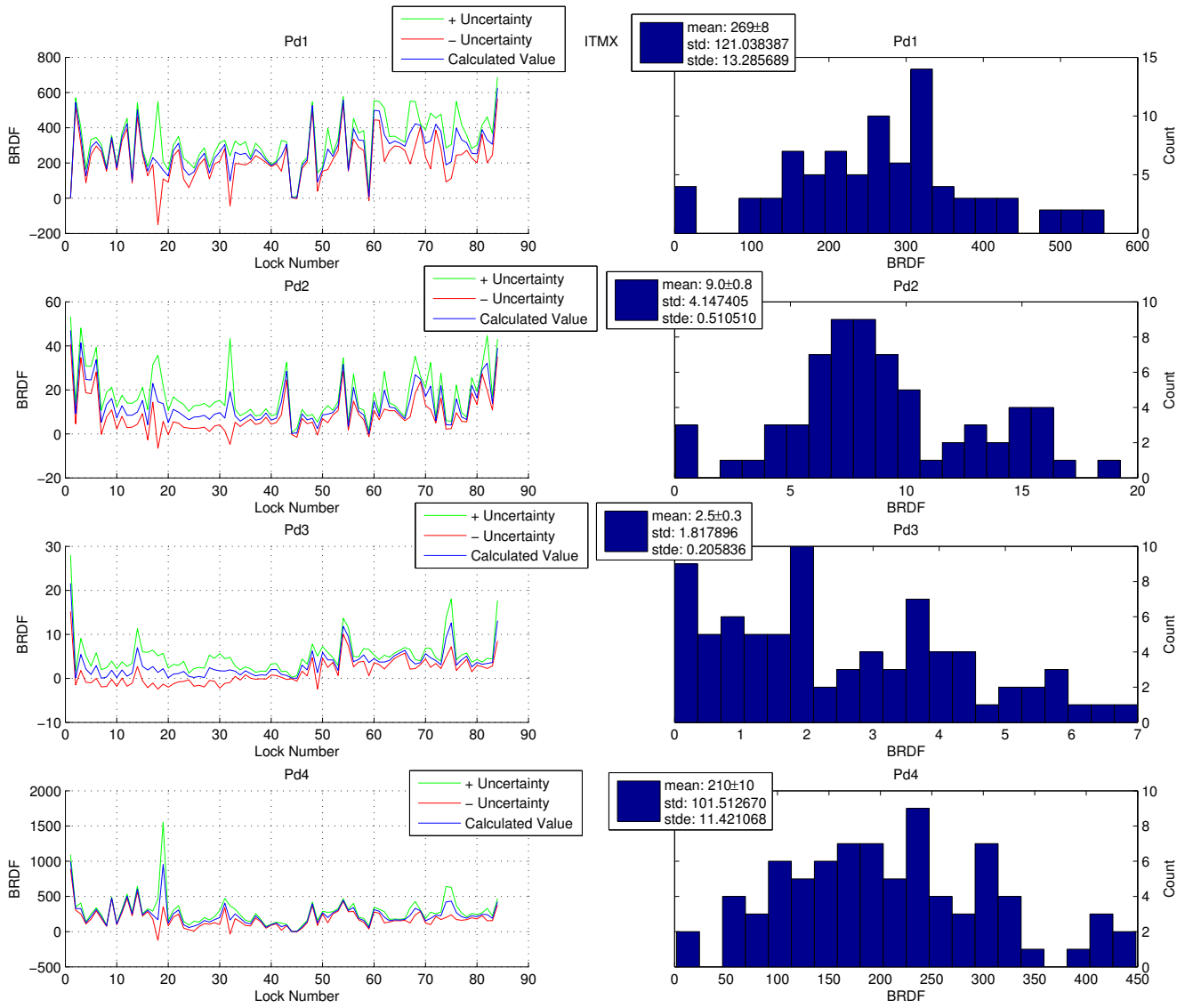

Figure 8: ITMX BRDFs and distribution by lock

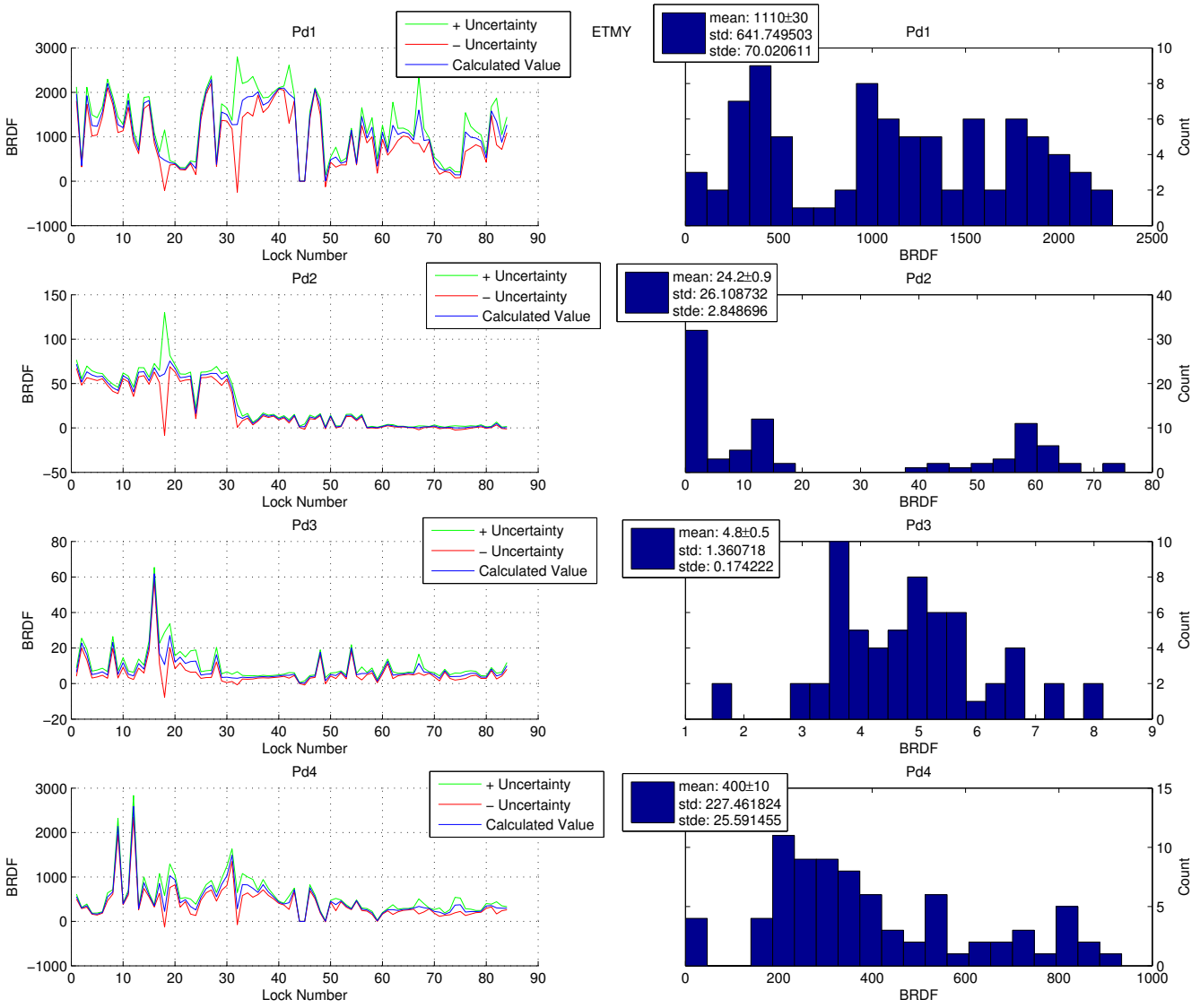

Figure 9: ETMY BRDFs and distribution by lock

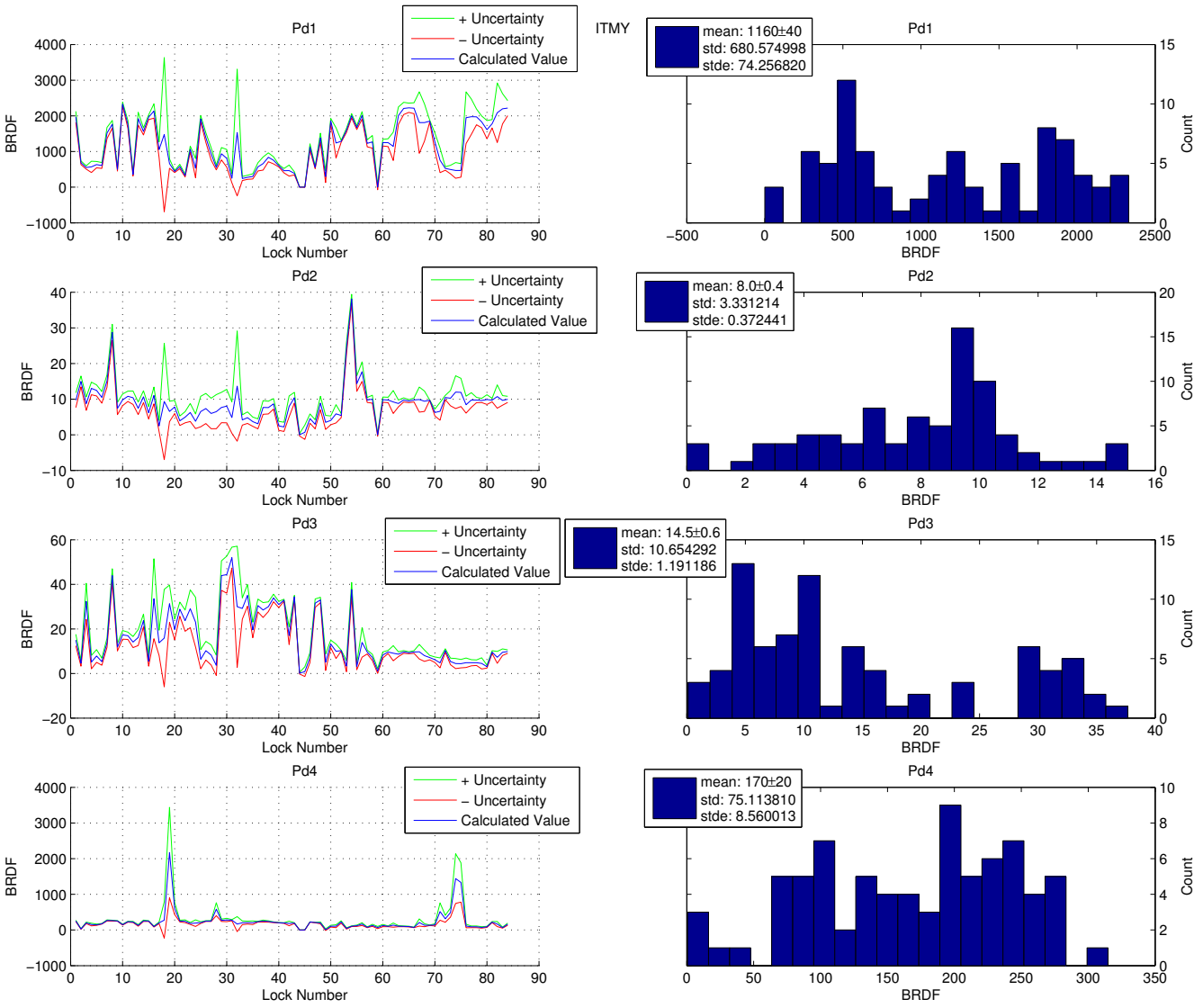

Figure 10: ITMY BRDFs and distribution by lock

Figures 7 through 10 show the BRDF values with uncertainty, as calculated from Equation 6, for each of the 84 locks in the left columns, and the distribution of values across all locks in the right columns. Standard deviations reach as high as 108% (Figure 9: ETMY PD2), while uncertainties in nearly all measurements remain below 20%. This could indicate systematic error or an unknown noise source. Figure 11 shows the cavity power for each arm during lock, along with uncertainties. Sudden peaks and troughs in this data tends to correlate with major fluctuations in the BRDFs, indicating that the PD voltages did not change with the power as expected. This could mean that these changes in power are not actually occurring.

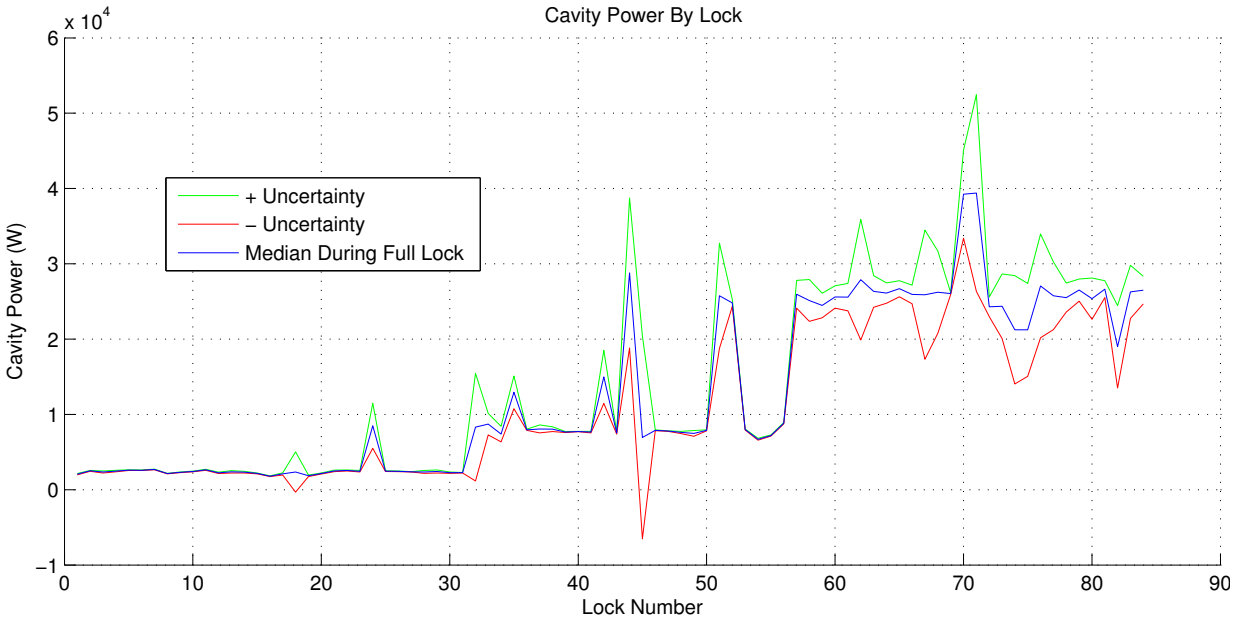

Figure 11: Cavity power for each lock as calculated from the power recycling pick off.

8 Modeling of Total Optical Scatter

8.1 Analysis of ETMY Image

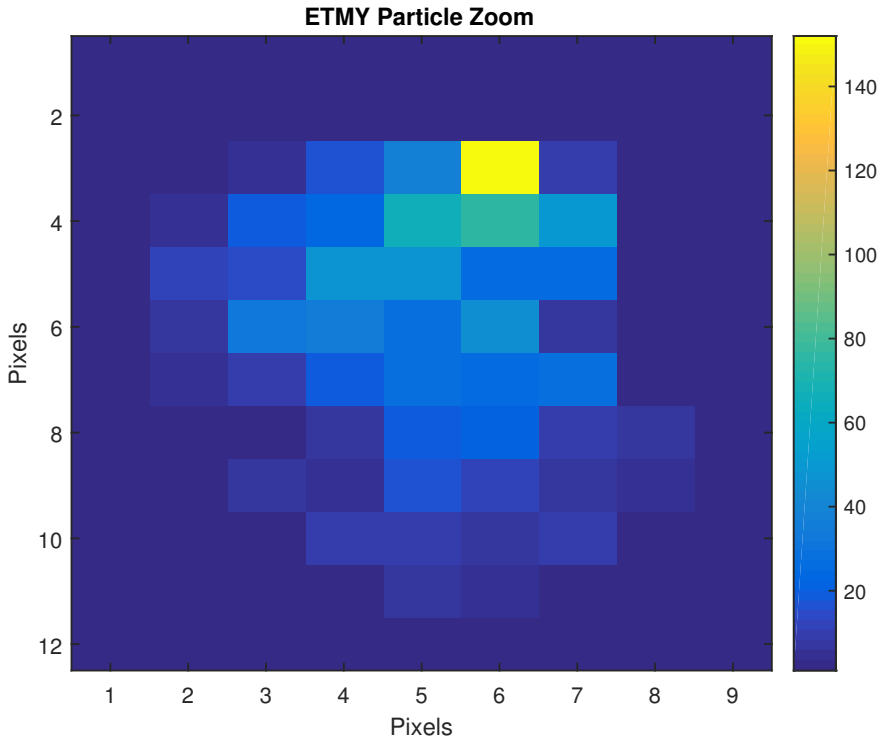

Figure 12: Zoom in of a particle seen on ETMY [4].

Figure 12 shows scatter from a particle on ETMY captured by a Basler ACE 100gm camera installed in a viewport of the IFO. The camera is roughly $5.8m$ from ETMY and at an angle of 10°, the lens diameter is $45mm$, and the image was taken at an exposure of $4\mu s$ [4]. From Equation 2, this gives a solid angle of 0.001 steradians. Using the 8-bit calibration factor of $1\times10^{-9}W\cdot\mu\cdot{p_i}^{-1}$, $1.3\times10^{-6}W$ are incident on the lens. Taking the cavity power to be $2500W$ and plugging these values into Equation 1, the BRDF is $1.1 \times 10^{-5}\ \Omega^{-1}$. Assuming 10° is a large enough angle to approximate the BRDF as constant, the total loss at that angle is simply given by $\pi \times BRDF$ [4]. This yields 3.6×10^{-5} or 36 ppm.

8.2 Stationary Interferometer Simulations

The path and power distribution ($W \times m^{-2}$) of the light in the IFO can be modeled using the Static Interferometer Simulation (SIS) package, which uses phase maps of the TMs taken *before installation*.

Figure 13: Model of power scattered to ITMY (looking towards the ITM).

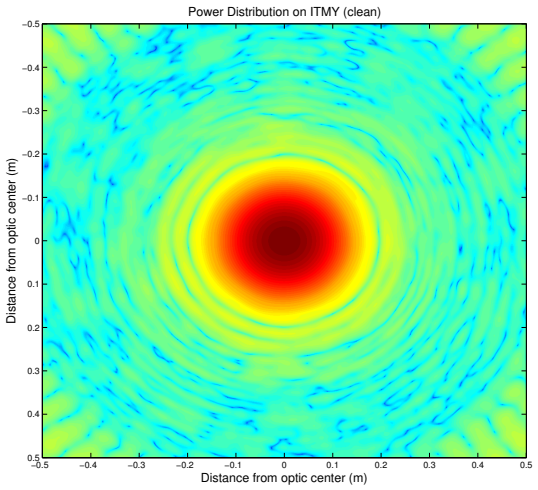

Figure 14: 3 Dimensional view of the model of power scattered to ITMY.

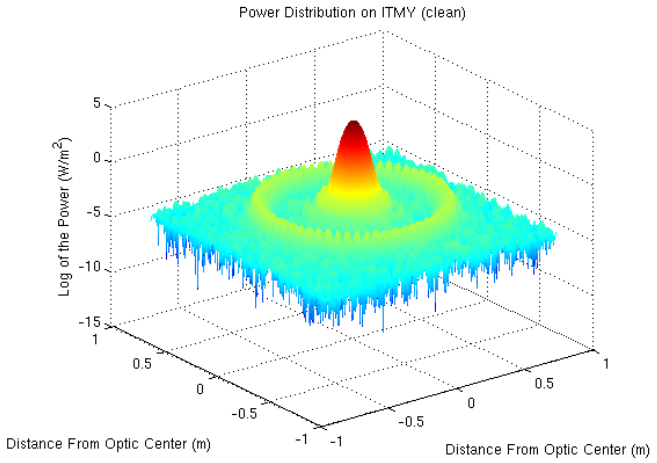

Figure 13 shows a head on view of this power distribution in log scale at ITMY. The features of peaks and troughs in the scattered power suggest that power measured by a PD could depend heavily on the alignment of the TMs. This might explain the large standard deviations seen in the PD BRDF measurements in Figures 7 through 10.

8.3 Comparison of Measured Data to the Model

Figure 15 shows how the measurements compare to the SIS modeled values for scatter towards ITMY. There are two important points to note from this plot:

- The measurements are comparable with the model
- Scatter from the installed TMs is larger than the model for all angles

The latter indicates that the fine structure of the TMs was altered during installation, likely from accumulation of particles.

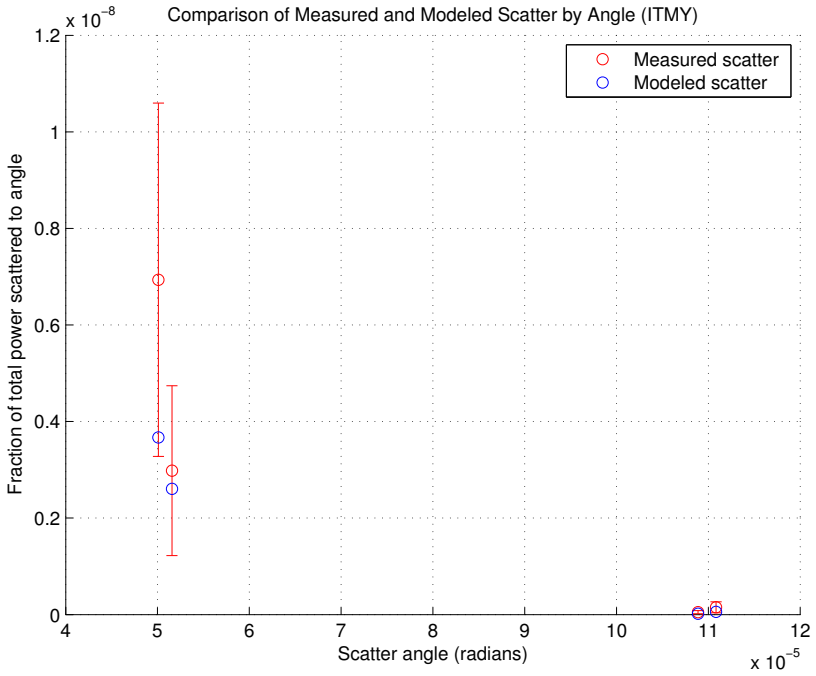

Figure 15: Measured and modeled fraction of power scattered to PDs.

In principle, the phase maps used by SIS can be altered to include any changes to the TM surfaces since installation. This, however, has proven very difficult to achieve and work is on going. Upon producing this updated model, one could integrate the power distribution across all angles to calculate the total power loss in each cavity, as well as where the power is going.

9 Conclusions and Future Work

Due to the sheer amount of samples and low uncertainties in measurements, we are confident that our findings do reflect the true mean BRDFs for each PD. We have begun comparing these measurements to models of optical scatter in the Fabry-Perot cavities based on phase maps of the clean TMs, using SIS. We have found that our measurements from the installed TMs are reasonable compared to the model. Our goal is to add modifications to these phase maps in an attempt to duplicate the particles that have accumulated on the TMs since installation. This will provide a model for the total scattering as it is today.

10 References

[1] Bsdf. http://en.wikipedia.org/wiki/File:BSDF05_800.png, 2006. File: BSDF05 800.png, GNU Free Documentation License.

[2] Joseph Betzwieser and Hunter Rew. Added temporary gige camera with power meter. https://alog.ligo-la.caltech.edu/aLOG/index.php?callRep=13151. LLO Logbook, Accessed: 07-07-2014.

[3] EG&G Photon Devices. *YAG Series*.

[4] Hunter Rew, Joseph Betzwieser, and David Feldbaum. Analysis of etmy scatter. https://alog.ligo-la.caltech.edu/aLOG/index.php?callRep=13414. LLO Logbook, Accessed: 07-07-2014.

[5] Manuel Ruiz and Tim Nguyen. *ACB 1 HOLE RIGHT QPD SKIN (w PD)*. LIGO DCC, October 2012.

[6] Peter R. Saulson. *Fundamentals of Interferometric Gravitational Wave Detectors*. World Scientific Publishing, 1994.

[7] John C. Stover. *Optical Scattering: Measurement and Analysis*. The International Society for Optical Engineering, second edition, 1995.

11 Acknowledgments

This research was conducted under Caltech's Summer Undergraduate Research Fellowship program at the Ligo Livingston Observatory and was funded by the National Science Foundation. Special thanks to Hiro Yamamoto of Caltech for his work on SIS and help with utilizing it for this research. I'd also like to thank my mentor, Joe, for constructing this project, as well as everyone at LLO who guided me through it.

Caltech